FEBS Letters 442 (1999) 138–142 FEBS 21388

Solution structure of the Eps15 homology domain of a human POB1 (partner of RalBP1)

Seizo Koshiba[a,b], Takanori Kigawa[a], Junji Iwahara[a], Akira Kikuchi[c], Shigeyuki Yokoyama[a,b,*]

[a] *Cellular Signaling Laboratory, The Institute of Physical and Chemical Research (RIKEN), 2-1 Hirosawa, Wako, Saitama 351-0198, Japan*
[b] *Department of Biophysics and Biochemistry, Graduate School of Science, The University of Tokyo, 7-3-1 Hongo, Bunkyo-ku, Tokyo 113-0033, Japan*
[c] *Department of Biochemistry, Hiroshima University School of Medicine, 1-2-3 Kasumi, Minami-ku, Hiroshima 734-8551, Japan*

Received 26 October 1998; received in revised form 2 December 1998

Abstract The solution structure of the Eps15 homology (EH) domain of a human POB1 (partner of RalBP1) has been determined by uniform $^{13}C/^{15}N$ labeling and heteronuclear multidimensional nuclear magnetic resonance spectroscopy. The POB1 EH domain consists of two EF-hand structures, and the second one binds a calcium ion. In the calcium-bound state, the orientation of the fourth α-helix relative to the other helices of the POB1 EH domain is slightly different from that of calbindin, and much more different from those of calmodulin and troponin C, on the basis of their atomic coordinates.

Key words: POB1; EH domain; Calcium-binding protein; Nuclear magnetic resonance; Solution structure

1. Introduction

The POB1 (partner of RalBP1) protein was originally identified as a protein that interacts with the Ral-binding protein 1 (RalBP1), a putative effector of a low-molecular-weight GTP-binding protein, Ral [1]. POB1 also binds to Grb2, becomes tyrosine-phosphorylated in response to epidermal growth factor (EGF), and makes a complex with the EGF receptor. The function of POB1 is not well known, but POB1 is thought to be an adapter protein that links a protein tyrosine kinase, a Src homology 3 (SH3) domain-containing protein, and Ral. POB1 consists of two proline-rich motifs, the coiled-coil region that interacts with RalBP1, and an Eps15 homology (EH) domain in the central region.

The EH domain was first identified as an internal repeat in Eps15, a substrate for the EGF receptor (EGFR) [2,3], and has now been found in many eukaryotic proteins from yeast to mammals [4]. Proteins with this domain are involved in endocytosis [5–9], actin cytoskeleton organization [5,6], and tyrosine kinase signaling pathways [1,10]. The EH domain has been reported to interact with proteins containing the Asn-Pro-Phe (NPF) motif, such as NUMB [11], RAB [11], synaptojanin [12], yAP180A [13], and epsin [14]. The EH domain consists of about 100 amino acid residues, and has sequence homology with EF-hand calcium-binding domains [2,3]. However, the binding of the EH domains of Eps15 to other proteins does not seem to be affected by the calcium concentration in vitro [3]. The POB1 EH domain has a high sequence homology with other EH domains. The POB1 EH domain has a calcium-binding site, while other EH domains have either one or none. In the present study, we determined the solution structure of the POB1 EH domain using heteronuclear multidimensional NMR spectroscopy. We also investigated calcium binding by the POB1 EH domain.

*Corresponding author. Fax: (81) (48) 462-4675.
E-mail: yokoyama@postman.riken.go.jp

Abbreviations: EGF, epidermal growth factor; EH, Eps15 homology; HSQC, heteronuclear single quantum coherence; NMR, nuclear magnetic resonance; NOE, nuclear Overhauser enhancement; NOESY, NOE spectroscopy; NPF, Asn-Pro-Phe; POB1, partner of RalBP1; RalBP1, Ral-binding protein 1; TOCSY, total correlated spectroscopy

2. Materials and methods

2.1. Protein expression and purification

The POB1 EH domain (residues 126–227) was expressed as a glutathione *S*-transferase (GST) fusion protein (Pharmacia Biotech Inc.). The uniformly ^{15}N- and $^{15}N/^{13}C$-labeled proteins were obtained by culture of *Escherichia coli* BL21 cells carrying this plasmid in M9 minimal medium supplemented with $MgSO_4$ (3 mM), $CaCl_2$ (300 μM), a trace element solution, a vitamin solution, ampicillin (0.06 mg/ml), and $^{15}NH_4Cl$ (1 g/l) as the sole nitrogen source and/or [$^{13}C_6$]D-glucose (3 g/l) as the sole carbon source. Harvested cells were suspended in 50 mM Tris-HCl buffer (pH 7.5) containing 100 mM NaCl, 5 mM $CaCl_2$, 2 mM DTT, 1 mM PMSF, and 0.1% (v/v) Triton, and were disrupted by sonication. After centrifugation, the supernatant was loaded onto a glutathione Sepharose 4B column (Pharmacia Biotech Inc.) equilibrated with 50 mM Tris-HCl buffer (pH 7.5) containing 100 mM NaCl, 5 mM $CaCl_2$, 2 mM DTT, and 1 mM PMSF. The bound proteins were eluted with the same buffer (pH 8.0) containing 15 mM glutathione (Sigma), and the fractions containing the fusion protein were concentrated with a Centriprep-10 unit (Amicon Inc.). The fusion protein was cleaved with thrombin (Sigma) for 1 h at 25°C, and then was applied to a DEAE Sephacel column (Pharmacia Biotech Inc.) equilibrated with 50 mM Tris-HCl buffer (pH 7.5) containing 5 mM $CaCl_2$ and 2 mM DTT. The bound proteins were eluted with an NaCl gradient (0–400 mM), and the fractions containing the EH domain were concentrated with Centriprep-3 and Centricon-3 units (Amicon Inc.). The protein was further purified by a FPLC Superdex 75 gel-filtration column (Pharmacia Biotech Inc.) equilibrated with 50 mM Tris-HCl buffer (pH 7.5) containing 150 mM NaCl, 5 mM $CaCl_2$, and 2 mM DTT. The fractions containing the EH domain were concentrated with a Centricon-3 unit (Amicon Inc.). The purity of the EH domain was verified by SDS-PAGE and mass spectrometry. The concentrations of the EH domain for the NMR analyses were 1.0 mM for the ^{15}N-labeled and 2.0 mM for the $^{15}N/^{13}C$-labeled samples, in 90% H_2O/10% ^2H_2O buffer containing 20 mM $^2H_6$ Tris-HCl (pH 7.5), 50 mM KCl, 5 mM $^2H_{10}$ DTT, 0.01% sodium azide, and 5 mM $CaCl_2$ for the ^{15}N-labeled and 10.0 mM $CaCl_2$ for the $^{15}N/^{13}C$-labeled samples.

2.2. NMR spectroscopy

All NMR experiments were performed at 303 K on a Bruker DRX600 spectrometer equipped with a triple resonance, pulse-field gradient probe. All spectra that detected NH magnetization were obtained using the water flip-back method [15]. The 2D ^1H-^{15}N HSQC [16], 3D ^{15}N-edited TOCSY-HSQC (37 ms mixing time) [17], ^{15}N-edited NOESY-HSQC (80 ms mixing time) [18], and HNHB [19]

PII: S0014-5793(98)01644-5

spectra were recorded for the ^{15}N-labeled sample. The 3D HNCA [20], HN(CO)CA [21], HNCO [20], HCACO [20], CBCANH [22], CBCA(CO)NH [23], HBHA(CO)NH [24], C(CO)NH [25], HCCH-TOCSY (20 ms mixing time) [26], HCCH-COSY [27], ^{13}C-edited NOESY-HSQC (100 ms mixing time) [28], 4D ^{13}C/^{15}N-edited NOESY (100 ms mixing time) [29], and ^{13}C/^{13}C-edited NOESY (100 ms mixing time) [30] spectra were also recorded for the ^{15}N/^{13}C-labeled sample. All spectra were processed on an Indigo2 IMPACT workstation (Silicon Graphics), using the NMRPipe system [31]. Analyses of the processed data were performed with the NMRView software package [32].

2.3. EDTA titration of the POB1 EH domain

The titration experiments of the POB1 EH domain with EDTA, using NMR analysis, were performed with 0.6 mM of the ^{15}N-labeled POB1 EH domain in 20 mM $^{2}H_6$ Tris-HCl buffer (pH 7.5) containing 50 mM KCl, 5 mM $^{2}H_{10}$ DTT, 0.01% sodium azide, and 3 mM $CaCl_2$. The 2D ^{1}H-^{15}N HSQC spectra were acquired at EDTA concentrations of 0, 1.0, 2.0, 2.5, 3.0, 3.6, and 6.0 mM.

2.4. Distance restraints

Interproton distance restraints were obtained from the 3D ^{15}N-edited NOESY-HSQC and ^{13}C-edited NOESY-HSQC spectra. The 4D ^{15}N/^{13}C-edited NOESY and ^{13}C/^{13}C-edited NOESY spectra were used only to identify the overlapped crosspeaks observed in the 3D spectra, and were not used for the calculation. The assigned nuclear Overhauser enhancements (NOEs) were classified into upper bound distance restraints of 2.9, 3.5, 4.5, and 5.5 Å for the NOEs from the ^{15}N-edited NOESY-HSQC spectrum, and 2.7, 3.3, 4.5, and 5.5 Å for the NOEs from the ^{13}C-edited NOESY-HSQC spectrum. The lower bounds for the interproton distance restraints were set to 1.8 Å. Distances involving methyl groups, aromatic ring protons, and non-stereospecifically assigned methylene protons were represented as $(\Sigma\, r^{-6})^{-1/6}$ sums [33]. The backbone hydrogen bond restraints were treated as previously described [34]. First, the secondary structure elements of the POB1 EH domain were determined by the NOE connectivities such as NH(i)-NH(i+1), H$^{\alpha}$(i)-NH(i+1), H$^{\alpha}$(i)-NH(i+2), H$^{\alpha}$(i)-NH(i+3), H$^{\alpha}$(i)-NH(i+4), and H$^{\alpha}$(i)-H$^{\beta}$(i+3) [35]. Then, the hydrogen bond restraints were given for the residue pairs that are involved in the secondary structure elements, and moreover exhibit no cross peak between NH and H_2O in the 3D ^{15}N-edited NOESY-HSQC spectrum measured by the water flip-back method. The upper and lower limits of the constraints for N-O were 3.5 and 2.5 Å, respectively, and those for NH-O were 2.5 and 1.5 Å, respectively. In addition, six distance restraints (2.0–2.8 Å) between the single calcium ion and the interacting oxygen atoms were included, based on the structures of other EF-hand proteins [36–41].

2.5. Dihedral angle restraints and stereospecific assignments

The ϕ and ψ dihedral angle restraints were given for the residues that are involved in the secondary structure elements determined by the NOE connectivities, and moreover have consistent chemical shift indices [42], as previously described [43]. In the α-helical regions, the ϕ and ψ angles were restrained to $-65°$ and to $-40°$ with allowed ranges of $\pm 30°$, respectively. In the β-sheet region, the ϕ and ψ angles were restrained to $-120°$ and to $130°$ with allowed ranges of $\pm 30°$, respectively. The χ^1 angle restraints were obtained from the 3D ^{15}N-edited HNHB, ^{15}N-edited TOCSY-HSQC, and ^{15}N-edited NOESY-HSQC spectra. The χ^1 angles were restrained to $-60°$ with allowed ranges of $\pm 30°$.

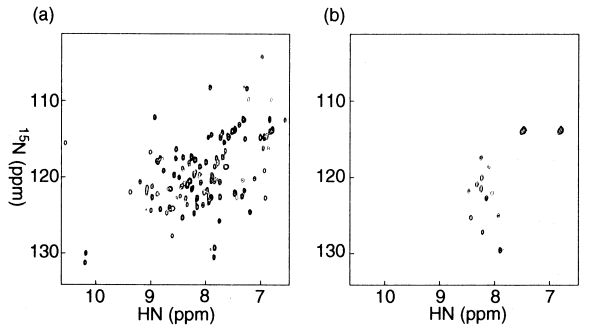

Fig. 1. ^{1}H-^{15}N HSQC NMR spectra of 0.6 mM of the uniformly ^{15}N-labeled POB1 EH domain with 3.0 mM $CaCl_2$, in the presence of (a) 0 mM EDTA and (b) 6.0 mM EDTA.

2.6. Structure calculations

Structures were calculated using the simulated annealing protocol [44] with X-PLOR 3.1 [45]. The final structure calculation was based on a total of 1527 restraints: 1444 interproton distance restraints (970 interresidue distance restraints), 22 distance restraints for 11 backbone hydrogen bonds, 61 dihedral angle restraints of 30 ϕ, 28 ψ, and three χ^1, and six distance restraints between the single calcium ion and the interacting oxygen atoms. All structure calculations were performed on an Indigo2 IMPACT workstation (Silicon Graphics).

3. Results and discussion

3.1. Calcium binding of the POB1 EH domain

As the EH domains have sequence homology with the EF-hand calcium-binding domains, we studied the calcium binding of the POB1 EH domain using EDTA titration. Fig. 1 shows the ^{1}H-^{15}N HSQC spectra of the POB1 EH domain with and without EDTA. Most of the peaks disappeared after the addition of 6 mM EDTA, indicating that the POB1 EH domain is tightly bound with Ca^{2+} and that the removal of Ca^{2+} results in denaturation or aggregation. The addition of calcium to this EDTA-treated solution failed to restore the initial spectrum (data not shown). Therefore, the denaturation (or aggregation) upon calcium removal is irreversible. Furthermore, gel-filtration and light-scattering experiments showed that the POB1 EH domain is in an aggregation state in the absence of Ca^{2+}, but is in a monomeric state in the presence of Ca^{2+} (data not shown). The second EF-hand calcium-binding motif of the POB1 EH domain has the conserved residues required for calcium binding, but the first motif does not, indicating that the POB1 EH domain binds only one calcium ion.

The EF-hand domains of calbindin and calmodulin have two calcium-binding sites per EF-hand domain [37,41], and their calcium-free states are stable enough for NMR analyses [46–49]. On the other hand, the POB1 EH domain has one calcium-binding site, and the dissociation of the calcium ion seems to make it very unstable. These data show that the calcium ion of the POB1 EH domain is necessary for the structure, and that the functions of the POB1 EH domain, which are still unknown, may not be regulated by the calcium concentration.

3.2. Resonance assignments

Sequence-specific assignments of the backbone, C$^{\beta}$, and H$^{\beta}$ resonances were obtained by analysis of the 3D HNCA, HN(CO)CA, HNCO, HCACO, CBCANH, CBCA(CO)NH, HBHA(CO)NH, ^{15}N-edited TOCSY, and ^{15}N-edited NOESY spectra. Of the 99 expected backbone amide resonances, 90 were observed in the ^{1}H-^{15}N HSQC spectrum of the POB1 EH domain. The missing peaks are those of the N-terminal six residues (Gly-1–Asn-6), the N-terminal residue of the second α-helix (Ser-42), the residue located in the loop between the second and third α-helices (Ile-55), and the residue located in the C-terminal extended region (Glu-96). These missing peaks are those of the residues exposed to the solvent as described below, indicating that the lack of these peaks is due to amide exchange with the solvent. The assignments of the aliphatic ^{1}H and ^{13}C resonances were mainly obtained from the 3D

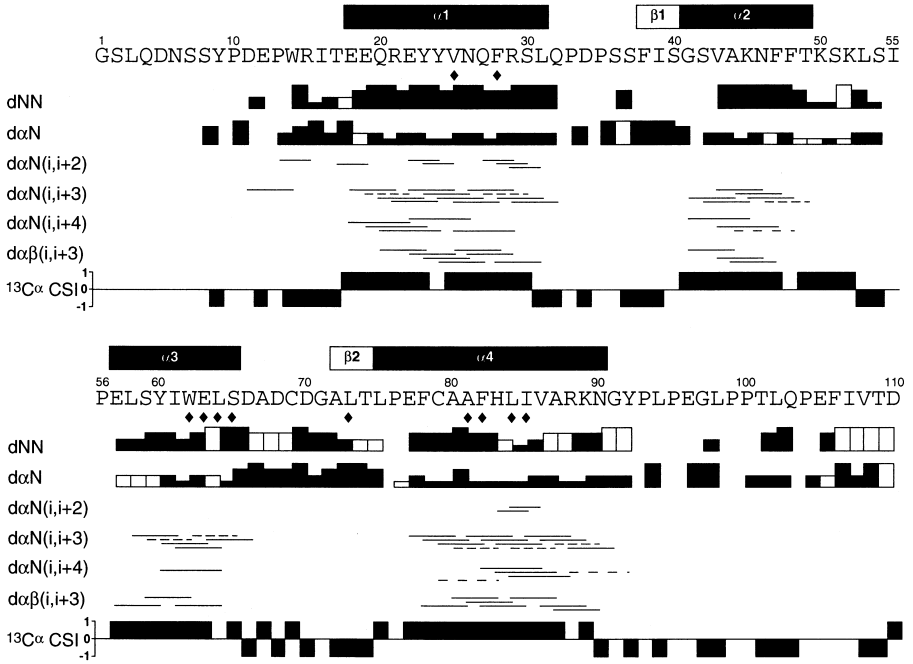

Fig. 2. Diagram of the sequential and medium-range NOE connectivities, the backbone hydrogen bonds, and the $^{13}C^{\alpha}$ chemical shift indices. The height of the bars reflects the strength of the NOE correlation, as strong, medium, weak, or very weak. The NOE connectivities that could not be established unambiguously because of overlaps are marked by open boxes (dNN and dαN) or dashed lines (dαN and dαβ). The residues that lacked a cross peak between the HN and H_2O resonances in the 3D ^{1}H-^{15}N NOESY-HSQC spectrum are indicated by ♦.

^{15}N-edited TOCSY, HCCH-TOCSY, HCCH-COSY, and C(CO)NH spectra, whereas those of the aromatic ring resonances were obtained from the 3D HCCH-COSY and ^{13}C-edited NOESY spectra.

3.3. Secondary structure determination

The secondary structure of the POB1 EH domain was determined on the basis of the 3D ^{15}N-edited and ^{13}C-edited NOESY spectra. The sequential and medium-range NOEs, the backbone hydrogen bonds, and the $^{13}C^{\alpha}$ chemical shift indices are summarized in Fig. 2. We identified four α-helices (α1–α4) and one short β-sheet (β1 and β2) in the secondary structure of the POB1 EH domain (Fig. 2).

3.4. Tertiary structure determination

The three-dimensional structure of the POB1 EH domain was determined from a total of 1527 restraints. The 18 final simulated-annealing structures satisfy the distance restraints, and have no violations greater than 0.3 Å and no dihedral angle violations greater than 3°. These structures were aligned by superimposing the backbone atoms (N, C^{α}, and C′) of the secondary structure elements, and are shown in Fig. 3a. The average root-mean-square (rms) deviation was 0.76 (±0.49) Å for the backbone atoms of the secondary structure elements (Table 1).

The sequence distribution of the intra- and interresidue NOE distance restraints is shown in Fig. 4. A number of interresidue NOEs were acquired for the secondary structure elements, although only a few interresidue NOEs were observed for the three loop regions (residues 32–37, 50–56, and 66–71) and for the N- and C-terminal regions (residues 1–17 and 91–110).

Fig. 3b shows a schematic ribbon diagram of the solution structure of the POB1 EH domain. This structure consists of a pair of helix-loop-helix (HLH) motifs, which make hydrophobic interactions, and their two loops constitute a short antiparallel β-sheet. The interhelical angle within the first HLH motif is much smaller than that within the second HLH motif. The three C-terminal α-helices (α2–α4) interact tightly with each other, and make a bundle structure. The second and fourth helices (α2 and α4) are nearly parallel, and the third helix (α3) is slightly tilted in comparison. On the other hand, the N-terminal α-helix (α1) is bound mainly to α4, with an angle of about 113° relative to α2 and α4. The calcium ion is located in the loop region of the second EF-hand motif.

The C-terminal region of the POB1 EH domain contains many proline residues, which are well conserved among EH

Table 1
Structural statistics of the 18 NMR structures

X-PLOR energies (kcal/mol)	
E_{total}	185 ± 10
E_{bond}	6.0 ± 0.8
E_{angle}	138 ± 6
$E_{improper}$	19 ± 2
E_{vdw}	9.5 ± 3.5
E_{noe}	13 ± 4
E_{cdih}	0.04 ± 0.17
E_{l-j}	−296 ± 64
rms deviations from idealized geometry	
Bonds (Å)	0.002 ± 0.000
Angles (°)	0.54 ± 0.011
Impropers (°)	0.37 ± 0.015
rms deviations from distance restraints	
All (Å)	0.014 ± 0.002
rms deviations from experimental dihedral angle restraints	
All (°)	0.08 ± 0.15
rms deviations about mean coordinate positions (Å)	
Secondary structure elements	
backbone (N, C^{α}, and C′)	0.76 ± 0.49
all non-H	1.19 ± 0.46

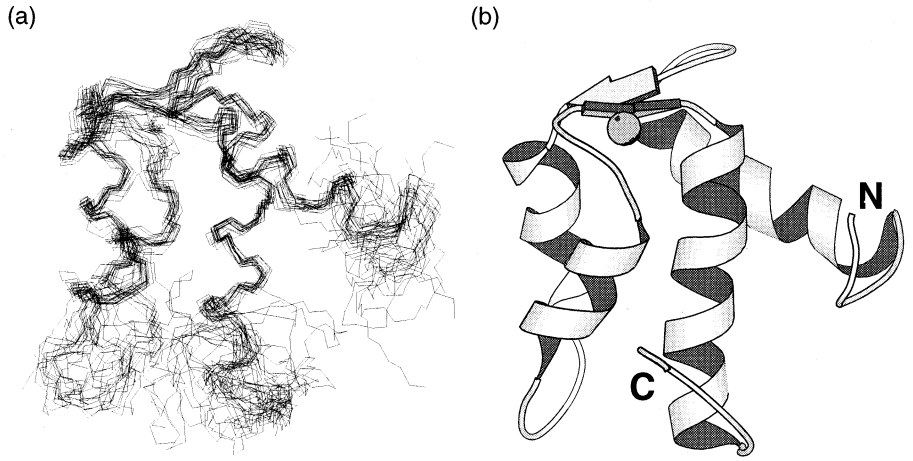

Fig. 3. a: The 18 backbone structures of the POB1 EH domain (residues 10–100), which were superimposed for the minimal rms deviation of the backbone atoms (N, C^{α}, and C′) of the secondary structure elements. This figure was generated using MIDASPlus [56]. b: Ribbon representation of the solution structure of the POB1 EH domain (residues 10–100). The amino- and carboxy-termini are indicated. The drawing was made with MOLSCRIPT [57].

domains. Some NOEs were observed between this proline-rich region and the second HLH motif, but the low number of restraints did not allow the structure of this proline-rich region to be determined well.

3.5. *Comparison of the structure of the POB1 EH domain with those of other EF-hand domains*

We compared the structure of the POB1 EH domain with those of other calcium-bound EF-hand proteins [37–39,41,50,51]. The secondary structure elements (four α-helices and two β-strands) and their topology within the POB1 EH domain are basically similar to those of other EF-hand domains. In more detail, the three-dimensional structure of the calcium-bound POB1 EH domain is similar to the closed conformation of calcium-bound calbindin [41], but is clearly different from the open conformations of calcium-bound calmodulin and troponin C [37–39]. Compared to the structure of calcium-bound calbindin, however, the fourth helix (α4) of the calcium-bound POB1 EH domain is more tightly packed with the third helix (α3). This interhelical angle (about 141°) seems to be similar to those of the solution structures of calcyclin and S100B [50,51], although the coordinates of these two proteins are not available. The sequences of the EH domains, especially the residues required for the hydrophobic core, are well conserved, indicating that these structural features are also conserved among the EH domains [1,3,4]. Furthermore, the EH domains recognize the Asn-Pro-Phe (NPF) motif [11–14], which is a different type of ligand recognition from those used by other EF-hand proteins [52–54]. Therefore, the EH domains constitute a distinct group within the EF-hand protein family.

During the preparation of this article, the structure and the peptide-binding site of the second EH domain (EH2) of Eps15 were reported [55]. The structure of the Eps15 EH2 domain

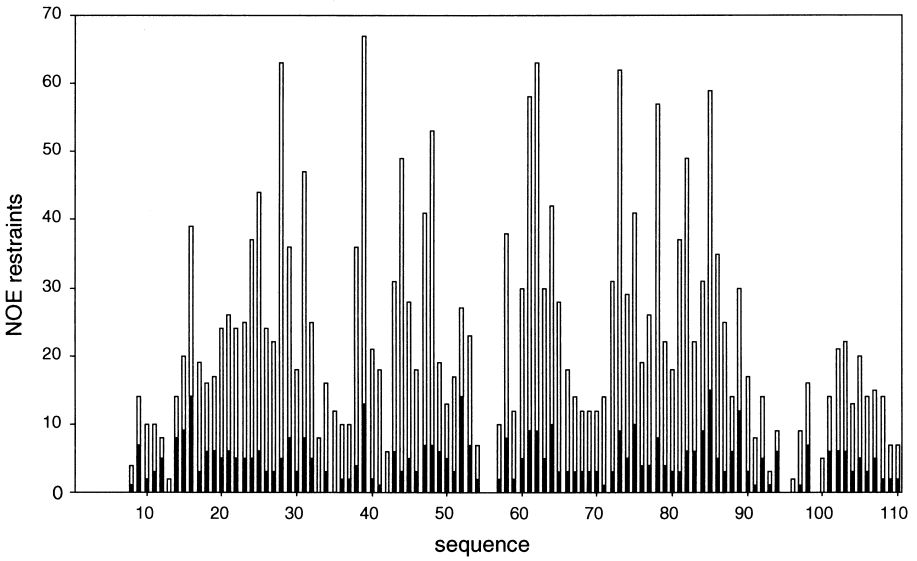

Fig. 4. The distribution of the NOE contacts in the POB1 EH domain as a function of the sequence position. Inter- and intraresidue NOEs are shown as open and filled boxes, respectively.

appears to be significantly similar to the POB1 EH domain, although the C-terminal proline-rich region of the Eps15 EH2 domain is tightly packed with the second EF-hand motif. This domain also binds one calcium ion in its second EF-hand motif. However, its calcium-free state was stable enough to be observed by NMR, whereas the calcium-free state of the POB1 EH domain was very unstable, suggesting that the calcium ion of the POB1 EH domain has a more critical role in structural stability than that of the Eps15 EH2 domain. The peptide-binding site of the Eps15 EH2 domain is located in the hydrophobic pocket between the second and third helices, which is different from the ligand-binding sites of other EF-hand proteins. The residues constituting this hydrophobic pocket are well conserved among the EH domains, including the POB1 EH domain, indicating that this binding mode is conserved.

Acknowledgements: We thank Drs. K. Takio and N. Domae for performing the mass spectrometry. We also thank Dr. M. Shirouzu for many helpful discussions. This work was supported by Grants-in-Aid from the Ministry of Education, Science, Sports and Culture, Japan.

References

[1] Ikeda, M., Ishida, O., Hinoi, T., Kishida, S. and Kikuchi, A. (1998) J. Biol. Chem. 273, 814–821.
[2] Fazioli, F., Minichiello, L., Matoskova, B., Wong, W.T. and Di Fiore, P.P. (1993) Mol. Cell. Biol. 13, 5814–5828.
[3] Wong, W.T., Schumacher, C., Salcini, A.E., Romano, A., Castagnino, P., Pelicci, P.G. and Di Fiore, P. (1995) Proc. Natl. Acad. Sci. USA 92, 9530–9534.
[4] Di Fiore, P.P., Pelicci, P.G. and Sorkin, A. (1997) Trends Biochem. Sci. 22, 411–413.
[5] Benedetti, H., Raths, S., Crausaz, F. and Riezman, H. (1994) Mol. Biol. Cell. 5, 1023–1037.
[6] Wendland, B., McCaffery, J.M., Xiao, Q. and Emr, S.D. (1996) J. Cell. Biol. 135, 1485–1500.
[7] Carbone, R., Fre, S., Iannolo, G., Belleudi, F., Mancini, P., Pelicci, P.G., Torrisi, M.R. and Di Fiore, P.P. (1997) Cancer Res. 57, 5498–5504.
[8] Benmerah, A., Lamaze, C., Begue, B., Schmid, S.L., Dautry-Varsat, A. and Cerf-Bensussan, N. (1998) J. Cell Biol. 140, 1055–1062.
[9] Roos, J. and Kelly, R.B. (1998) J. Biol. Chem. 273, 19108–19119.
[10] Yamaguchi, A., Urano, T., Goi, T. and Feig, L.A. (1997) J. Biol. Chem. 272, 31230–31234.
[11] Salcini, A.E. et al. (1997) Genes Dev. 11, 2239–2249.
[12] Haffner, C. et al. (1997) FEBS Lett. 419, 175–180.
[13] Wendland, B. and Emr, S.D. (1998) J. Cell Biol. 141, 71–84.
[14] Chen, H., Fre, S., Slepnev, V.I., Capua, M.R., Takei, K., Butler, M.H., Di Fiore, P.P. and De Camilli, P. (1998) Nature 394, 793–797.
[15] Grzesiek, S. and Bax, A. (1993) J. Am. Chem. Soc. 115, 12593–12594.
[16] Bodenhausen, G. and Ruben, D.J. (1980) Chem. Phys. Lett. 69, 185–189.
[17] Marion, D., Driscoll, P.C., Kay, L.E., Wingfield, P.T., Bax, A., Gronenborn, A.M. and Clore, G.M. (1989) Biochemistry 28, 6150–6156.
[18] Marion, D., Kay, L.E., Sparks, S.W., Torchia, D.A. and Bax, A. (1989) J. Am. Chem. Soc. 111, 1515–1517.
[19] Archer, S.J., Ikura, M., Torchia, D.A. and Bax, A. (1991) J. Magn. Reson. 95, 636–641.
[20] Kay, L.E., Ikura, M., Tschudin, R. and Bax, A. (1990) J. Magn. Reson. 89, 496–514.
[21] Bax, A. and Ikura, M. (1991) J. Biomol. NMR 1, 99–104.
[22] Grzesiek, S. and Bax, A. (1992) J. Magn. Reson. 99, 201–207.
[23] Grzesiek, S. and Bax, A. (1992) J. Am. Chem. Soc. 114, 6291–6293.
[24] Grzesiek, S. and Bax, A. (1993) J. Biomol. NMR 3, 185–204.
[25] Grzesiek, S., Anglister, J. and Bax, A. (1993) J. Magn. Reson. Ser. B 101, 114–119.
[26] Bax, A., Clore, G.M. and Gronenborn, A.M. (1990) J. Magn. Reson. 88, 425–431.
[27] Ikura, M., Kay, L.E. and Bax, A. (1991) J. Biomol. NMR 1, 299–304.
[28] Muhandiram, D.R., Farrow, N.A., Xu, G.Y., Smallcombe, S.H. and Kay, L.E. (1993) J. Magn. Reson. Ser. B 102, 317–321.
[29] Kay, L.E., Clore, G.M., Bax, A. and Gronenborn, A.M. (1990) Science 249, 411–414.
[30] Vuister, G.W., Clore, G.M., Gronenborn, A.M., Powers, R., Garrett, D.S., Tschudin, R. and Bax, A. (1993) J. Magn. Reson. Ser. B 101, 210–213.
[31] Delaglio, F., Grzesiek, S., Vuister, G.W., Zhu, G., Pfeifer, J. and Bax, A. (1995) J. Biomol. NMR 6, 277–293.
[32] Johnson, B.A. and Blevins, R.A. (1994) J. Biomol. NMR 4, 603–614.
[33] Nilges, M. (1993) Proteins 17, 297–309.
[34] Iwahara, J., Kigawa, T., Kitagawa, K., Masumoto, H., Okazaki, T. and Yokoyama, S. (1998) EMBO J. 17, 827–837.
[35] Wüthrich, K. (1986) NMR of Proteins and Nucleic Acids, John Wiley and Sons, New York.
[36] McPhalen, C.A., Strynadka, N.C. and James, M.N. (1991) Adv. Protein Chem. 42, 77–144.
[37] Chattopadhyaya, R., Meador, W.E., Means, A.R. and Quiocho, F.A. (1992) J. Mol. Biol. 228, 1177–1192.
[38] Herzberg, O. and James, M.N. (1988) J. Mol. Biol. 203, 761–779.
[39] Strynadka, N.C., Cherney, M., Sielecki, A.R., Li, M.X., Smillie, L.B. and James, M.N. (1997) J. Mol. Biol. 273, 238–255.
[40] Declercq, J.P., Tinant, B., Parello, J. and Rambaud, J. (1991) J. Mol. Biol. 220, 1017–1039.
[41] Svensson, L.A., Thulin, E. and Forsen, S. (1992) J. Mol. Biol. 223, 601–606.
[42] Wishart, D.S. and Sykes, B.D. (1994) J. Biomol. NMR 4, 171–180.
[43] Bagby, S., Kim, S., Maldonado, E., Tong, K.I., Reinberg, D. and Ikura, M. (1995) Cell 82, 857–867.
[44] Nilges, M., Kuszewski, J. and Brünger, A.T. (1991) in: Computational Aspect of the Study of Biological Macromolecules by NMR (Hoch, J.C., Ed.), Plenum Press, New York.
[45] Brünger, A.T. (1993) X-PLOR Version 3.1: A System for X-ray Crystallography and NMR, Yale University Press, New Haven, CT.
[46] Skelton, N.J., Kordel, J. and Chazin, W.J. (1995) J. Mol. Biol. 249, 441–462.
[47] Zhang, M., Tanaka, T. and Ikura, M. (1995) Nature Struct. Biol. 2, 758–767.
[48] Kuboniwa, H., Tjandra, N., Grzesiek, S., Ren, H., Klee, C.B. and Bax, A. (1995) Nature Struct. Biol. 2, 768–776.
[49] Finn, B.E., Evenas, J., Drakenberg, T., Waltho, J.P., Thulin, E. and Forsen, S. (1995) Nature Struct. Biol. 2, 777–783.
[50] Smith, S.P. and Shaw, G.S. (1998) Structure 6, 211–222.
[51] Sastry, M., Ketchem, R.R., Crescenzi, O., Weber, C., Lubienski, M.J., Hidaka, H. and Chazin, W.J. (1998) Structure 6, 223–231.
[52] Crivici, A. and Ikura, M. (1995) Annu. Rev. Biophys. Biomol. Struct. 24, 85–116.
[53] Vassylyev, D.G., Takeda, S., Wakatsuki, S., Maeda, K. and Maeda, Y. (1998) Proc. Natl. Acad. Sci. USA 95, 4847–4852.
[54] Schafer, B.W. and Heizmann, C.W. (1996) Trends Biochem. Sci. 21, 134–140.
[55] de Beer, T., Carter, R.E., Lobel-Rice, K.E., Sorkin, A. and Overduin, M. (1998) Science 281, 1357–1360.
[56] Ferrin, T.E., Huang, C.C., Jarvis, L.E. and Langridge, R. (1988) J. Mol. Graphics 6, 13–27.
[57] Kraulis, P.J. (1991) J. Appl. Crystallogr. 24, 946–950.